A coarse grain model for *n*-alkanes parameterized from surface tension data

Steve O. Nielsen, Carlos F. Lopez, Goundla Srinivas, and Michael L. Klein[a)]
Center for Molecular Modeling and Department of Chemistry, University of Pennsylvania, Philadelphia, Pennsylvania 19104-6323

(Received 30 June 2003; accepted 18 July 2003)

Molecular dynamics simulations are carried out in a systematic manner to develop a coarse grain model for multiple-of-three carbon *n*-alkanes. The procedure involves optimizing harmonic bond and bend parameters, and Lennard-Jones nonbonded parameters, to match observables taken from fully atomistic simulations and from experiment. The experimental values used consist of surface tension and bulk density data. Scaling relations are introduced to allow for the representation of the remaining *n*-alkanes. As *n* increases these relations converge to the multiple-of-three carbon values. The model is assessed by comparing it to both fully atomistic simulation and experimental data which was not used in the fitting procedure. © *2003 American Institute of Physics.*
[DOI: 10.1063/1.1607955]

I. INTRODUCTION

Despite the relentless increase in computational throughput, significant effort is being devoted towards developing techniques that further enhance the time and length scales accessible in molecular simulations. This effort is aimed at bridging the still large gap between simulations and the time and length scales of typical biological events as observed by experiment, such as raft formation in membranes.[1] These techniques come in two flavors. The first involves biasing the simulation to study a particular event of interest; for example the unfolding of a protein.[2] The fast growth method of Jarzynski[3] and its implementation by Schulten as steered molecular dynamics[4] represent a recent advance in this area. The second, and the focus of the current work, is to remove detail by coarse graining.[5] These two sets of techniques are not mutually exclusive—for instance, the potential of mean force between two membrane inclusions[6] could be constructed by using umbrella sampling in a coarse grain simulation.

There are several consequences in moving from a fully atomistic description to a coarse grained one. It is well known that all models which use *effective* pair potentials, including condensed phase all-atom (AA), united-atom (UA), and coarse grain (CG) force fields, are thermodynamically inconsistent.[7,8] Louis[7] concludes that at best, a force field which uses effective pair potentials can be chosen to perform well for some particular physical properties of interest. In this respect AA and CG models are on the same footing. However, CG models usually make use of atomic-level pair correlation functions, either from atomistic simulations[9] or from experiment,[10] as data to parameterize against. This strategy has the advantage that detailed structural information is incorporated into the CG model, but suffers from a loss of transferability; since the radial distribution function incorporates temperature, density, composition, and other dependencies into the effective pair interaction, the resulting force field can have a severely limited range of applicability.[11]

Recent CG *n*-alkane (polyethylene) models use structural data from atomistic simulations to develop the force field.[8,12,13] For polymeric systems in general, the strategy has been to use radial distribution functions from atomistic simulations, sometimes in combination with thermodynamic data, to determine the CG force field.[14] The thermodynamic data utilized is invariably bulk density and vapor pressure.[14,15] The use of vapor pressure stems from its ubiquity in AA force field development and because large compendiums of data are available.

Our aim is of a different nature. We are interested in improving upon an existing model for aqueous amphiphilic systems which consists of water, alkane, and 1,2-di-*n*-alkanoyl-*sn*-glycero-3-phosphocholine parameters which has been successfully applied in numerous studies.[15–19] Consequently, the alkane model we are developing will eventually be used as the hydrophobic part of amphiphiles such as phospholipids and alkyl sulfonates. The alkane chains in these partially ordered systems are arranged quite differently than in purely hydrophobic liquids; this difference would be manifested in the radial distribution functions for the alkane chains. The hydrophobic segments in aqueous amphiphilic systems are generally involved in nonspecific interactions and hence it should be possible to have an alkane model which is suitable for a wide range of systems. The hydrophilic head groups of the amphiphiles can be tuned for specific environments to reflect the local hydrogen bonding and solvation shell structure.[15] For generality we chose a Lennard-Jones form for the intermolecular potentials. Since the driving force for self-assembly in aqueous amphiphilic systems is the segregation of hydrophobic and hydrophilic regions, an essential ingredient in models of these systems is to have the correct interfacial tension. The analogous interfacial quantity for pure alkane systems is the liquid/air sur-

a)Electronic mail: klein@cmm.upenn.edu; URL: www.cmm.upenn.edu

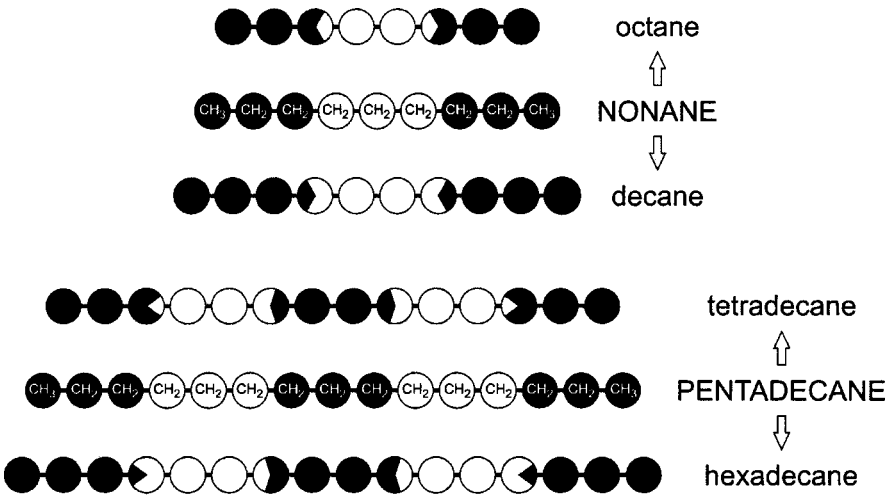

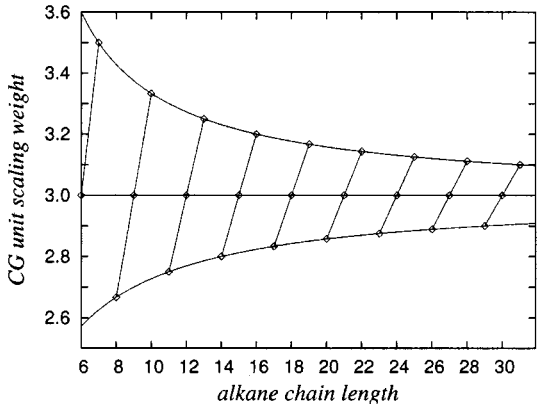

FIG. 1. Coarse graining conceptualization. For multiple-of-three carbon alkanes, three consecutive carbon atoms and their associated hydrogen atoms are represented by one CG site, as shown for nonane and pentadecane by the black and white regions. For all other chain lengths, the number of CG sites used in their representation is that of the nearest multiple-of-three alkane. Three sites represent octane and decane as shown schematically by the blocks of black and white shading, with each site having a weight of 8/3 and 10/3, respectively, as shown in the plot and as described in the text. Similarly, tetradecane and hexadecane are represented by five sites of weight 14/5 and 16/5, respectively, as shown. Note that as the chain length becomes long, the scaling weights all converge to three.

face tension. Experimental bulk density and surface tension of the *n*-alkanes at 303 K is used to determine the Lennard-Jones parameters.

II. METHODS

The CHARMM AA force field was used to perform molecular dynamics simulations of the bulk phase for each of the *n*-alkanes from hexane to octadecane with 200 molecules. Short runs sufficed because only intramolecular data from these AA simulations was used in the CG parameterization. The simulations were extended to 500 ps for hexane, heptane, nonane, dodecane, tetradecane, and octadecane to obtain better statistics on their bulk properties. CG molecular dynamics simulations were run with between 1000 and 1500 molecules for each of the *n*-alkanes from hexane to octadecane in both bulk and slab[20] geometries. In addition, four large CG bulk systems where simulated, corresponding to $C_{21}H_{44}$, $C_{27}H_{56}$, $C_{39}H_{80}$, and $C_{63}H_{128}$. The slab geometry is used with three-dimensional periodic boundary conditions to facilitate the computation of Ewald sums and hence contains two liquid/vacuum interfaces. The bulk systems were run for 2.5 ns each and the slab systems for between 25 and 40 ns each; these times are not equivalent to AA times as will be discussed below.[13,18] Since the intermolecular and intramolecular properties are almost independent of one another, a crude set of intermolecular parameters were used while refining the intramolecular parameters. Subsequently the intermolecular parameters were refined; near the end of this procedure the intramolecular properties were calculated to see if they had been affected and minor adjustments were made. The bulk AA and CG runs were performed in an orthorhombic NPT ensemble at 1 atm and 303 K; the slab runs were performed in the NVT ensemble at 303 K. The instantaneous surface tension is computed as

$$\gamma_{\text{inst}} = \frac{L_z}{2}\left(P_{zz} - \frac{P_{xx}+P_{yy}}{2} \right), \tag{1}$$

where the first factor of 1/2 is included to account for the two interfaces in the simulation box, L_z is the box size in the *z*-direction, and P_{ij} is the ij component of the pressure tensor. The interfacial plane is the xy plane.

III. MODEL CONSTRUCTION

In the present model, the CG *n*-alkanes are constructed from terminal (T) and middle (M) chain units. These units interact through a Lennard-Jones 9-6 nonbonded potential,

$$V(r) = (27\epsilon/4)[(\sigma/r)^9 - (\sigma/r)^6], \tag{2}$$

and through harmonic bond and bend intramolecular potentials

$$V_{\text{bond}} = (k/2)(r - r_{\text{eq}})^2; \quad V_{\text{bend}} = (k/2)(\theta - \theta_{\text{eq}})^2. \tag{3}$$

TABLE I. Parameters for the weight three interactions. The bond and bend potentials are harmonic [see Eq. (3)] and the Lennard-Jones potential is given in Eq. (2). The Lennard-Jones *TM* parameters are given by the Lorenz–Bertholot mixing rules. The scaling used to obtain the remaining interactions is given in the text.

Bond parameters		
Sites	k (K)	r_{eq} (Å)
TT	7000	3.71
TM	6200	3.65
MM	6200	3.64
Bend parameters		
Sites	k (K)	θ_{eq} (deg)
TMT	1100	175.5
TMM	1200	175.0
MMM	1200	173.0
Lennard-Jones parameters		
Sites	ϵ(K)	σ(Å)
TT	218.9	4.662
MM	195.8	4.582

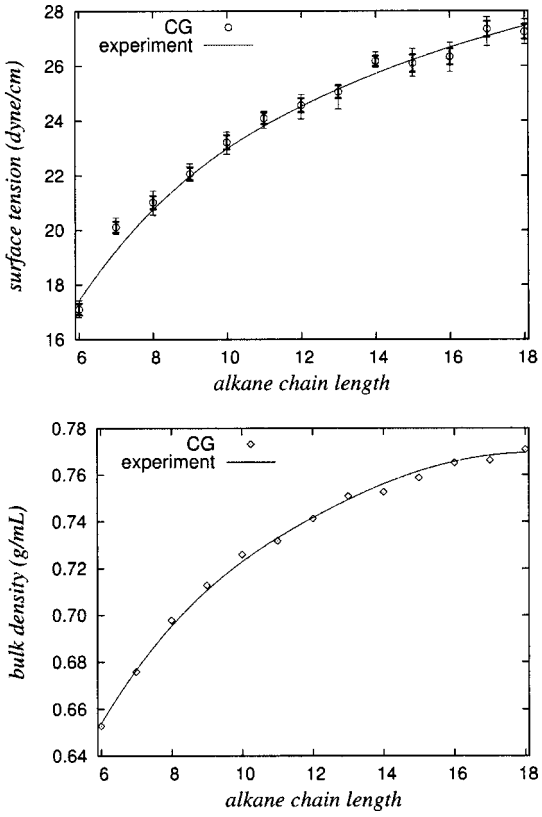

FIG. 2. Experimental and CG density and surface tension. The experimental data has been splined for clarity. The error bars on the CG surface tension data are as follows. The instantaneous surface tension time series is partitioned into ten equal segments and the mean is computed for each segment. The minimum and maximum of these ten means are plotted as the outer, thin set of error bars. The standard deviation of these means constitute the inner, thick error bars.

The current CG model, as in AA and UA models, does not explicitly rule out chain crossing in the manner of Briels and Padding.[21] This is because the CG unit of Briels and Padding encompasses 20 monomers. As pointed out by Fukunaga,[12] the current CG unit is small enough for crossing not to be a concern. The parameters for these potentials are determined as follows.

First, target data is obtained. The target data for the intramolecular potentials is calculated from AA simulations and consists of the mean and standard deviation of distances and angles between the CG sites, which are obtained from the AA data in the following manner. The number of carbon atoms in the alkane chain, n_{AA} is divided by three and the result is rounded to the nearest integer; this gives the number of sites in the CG representation, n_{CG}. The number of carbon atoms divided by the number of CG sites gives the scaling weight, $w = n_{AA}/n_{CG}$, of each CG site (see Fig. 1). Note that by giving each site the same weight we are spreading the ''extra'' carbon atoms (the number of carbon atoms modulo three) uniformly over the entire molecule. Starting at one end of the AA alkane chain, we count out w carbon atoms. The center of mass of these atoms along with their associated hydrogen atoms determines the location of the first CG site. Fractional atoms are given a reduced mass in the center-of-mass calculation. To assign the second CG site a further w carbon atoms are marked off. If the counting begins at a fractional site, the remainder of that site is used. This procedure is illustrated in Fig. 1. The target data used for the nonbonded interactions consists of bulk density and surface tension experimental data.

CG simulations are initially carried out using an existing parameter set.[15] The parameter refinement is done in a systematic fashion by initially restricting ourselves to alkane chains with a multiple of three carbon atoms. The terminal–terminal (TT) harmonic bond parameters, which only exist for hexane, are determined by matching the mean and standard deviation between bulk CG hexane and the AA target data. The parameters for the *TM* and *MM* bonds were set by demanding close agreement between the mean and standard deviation from bulk CG simulations of nonane, dodecane, pentadecane, and octadecane with the AA target data for the same group of molecules. The *TMT* bend parameters, which only exist for nonane, are determined by matching the mean and standard deviation between bulk CG nonane and the AA target data. The parameters for the *TMM* and *MMM* bends were set by demanding close agreement between the mean and standard deviation from bulk CG simulations of dodecane, pentadecane, and octadecane with the AA target data for the same group of molecules. The target bond potentials have two minima corresponding to the bent and extended configurations.[12] This shape arises from correlations with other degrees of freedom. Fully reproducing the distribution in the CG representation changes the nature of the barrier between the minima from having a dynamical origin to having only a statistical one; for simplicity we have chosen to approximate the distribution as unimodal because we are not concerned with this level of detail.

For the nonbonded parameters, we begin with the CG hexane system which is composed entirely of terminal units. By demanding that the bulk system yields the correct experimental density, and that the slab system yields the correct experimental surface tension, the values for ϵ_{TT} and σ_{TT} are obtained. To determine the remaining nonbonded param-

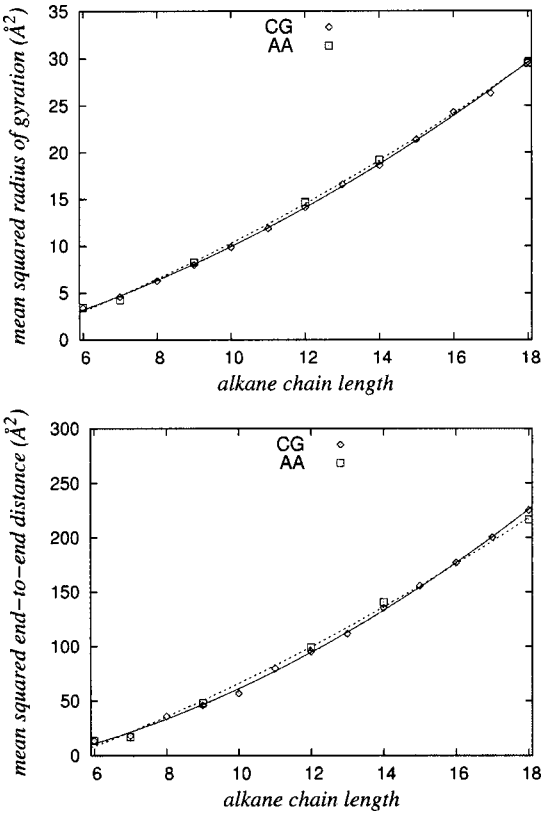

FIG. 3. Mean squared radius of gyration and mean squared end-to-end distance as a function of alkane chain length. The all-atom data is analyzed using the coarse grain reduction procedure. The best quadratic fit to the data is also shown.

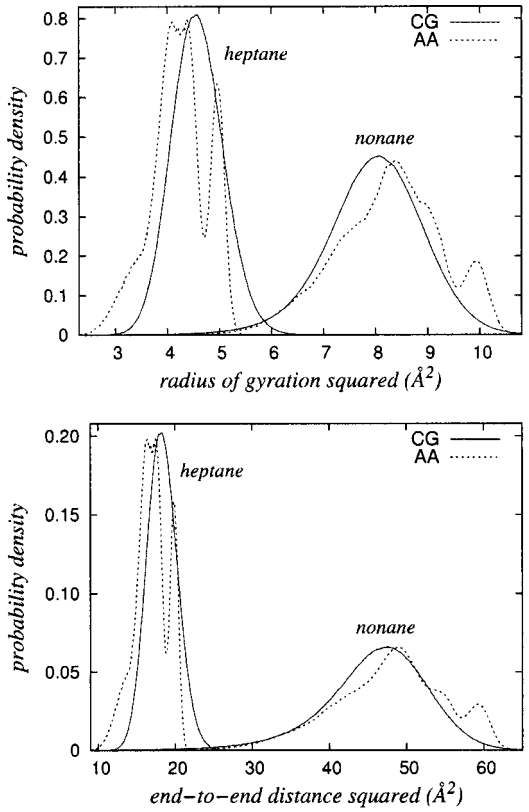

FIG. 4. The full distribution of the data from Fig. 3 is shown for heptane and nonane. The all-atom data is analyzed using the coarse grain reduction procedure.

eters, the cross terms, ϵ_{TM} and σ_{TM}, are fixed from the Lorenz–Bertholot mixing rules[22] and the values of ϵ_{MM} and σ_{MM} are obtained by simulating bulk and slab geometries for nonane, dodecane, pentadecane, and octadecane, and demanding a close match between the density and surface tension for this series of CG molecules compared to experiment. This finishes the parameterization task for the multiple-of-three alkanes (see Table I).

The nonbonded parameter adjustment was facilitated by doing a series of CG simulations around the base value of $\epsilon_{\mathrm{TT}}=218.9\,\mathrm{K}$, $\epsilon_{MM}=195.8\,\mathrm{K}$, $\sigma_{\mathrm{TT}}=4.662\,\text{Å}$, $\sigma_{MM}=4.582\,\text{Å}$ (with the *TM* values given by the Lorenz–Bertholot combination rules) to map out, locally, the iso-density and iso-surface tension contours in parameter space. As expected, the iso-density contour lies close to the ϵ-axis and the iso-surface tension contour lies close to the σ axis. Their exact location allows for the surface tension to be adjusted independently from the density.

IV. SCALING

So far we have chosen to group three consecutive carbon atoms and their associated hydrogen atoms into one CG site.[12,15] Three possibilities to treat chains of arbitrary length are now discussed.

First, the problem could be ignored and the length restricted to multiple-of-three carbon atoms. This is unnecessarily restrictive—for example, the commonly used surfactants dimyristoylphosphatidylcholine (DMPC) and dipalmitoylphosphatidylcholine (DPPC) are both desirable to have for CG studies, but their hydrophobic tails differ by two carbons in length, being 14 and 16 carbon atoms long, respectively. Even worse, phospholipids with an odd number of alkanoyl carbon atoms are rarely found in nature.

Second, a smaller, two-carbon, unit could be introduced. Since the greatest common divisor of two and three is one, any length chain could then be built. This choice, however, leads to an unphysical representation of the chain. One could imagine a model with a gradation of sizes as one progresses inwards towards the middle of the chain, but to have an oversized knob or an undersized dimple interrupt this smooth progression has no physical basis, i.e., no basis in the underlying structure of the molecule. Having sudden changes in the size of units along a polymer chain might not overly distort the properties of an isotropic bulk or melt phase, but would be expected to lead to pathological behavior in liquid crystalline states because of the partial order and alignment present in such systems.

In what follows we introduce scaling relations to avoid such unphysical size discrepancies along the chain. The number of sites in the CG representation is not changed from the closest multiple of three. The scaling is done on the CG alkanes $C_{3n}H_{9n+2}$ to mimic the alkanes $C_{3(n\pm1/3)}H_{9(n\pm1/3)+2}$. Since the modification is spread uniformly over the entire chain, each site of a CG chain with n sites should be subject to a scaling ratio of roughly $1\pm1/3n$ (see Fig. 1). Scaling is performed on the mass, the

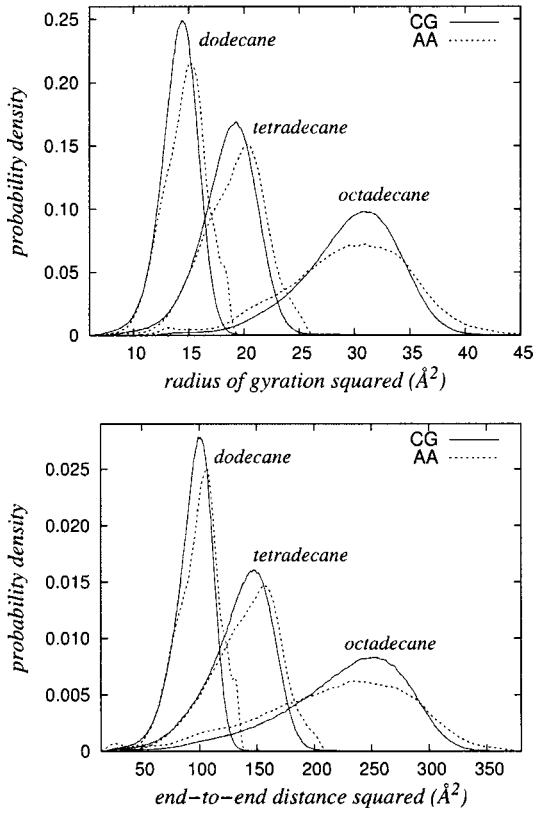

FIG. 5. The full distribution of the data in Fig. 3 is shown for dodecane, tetradecane, and octadecane. The all-atom data is analyzed using the coarse grain reduction procedure.

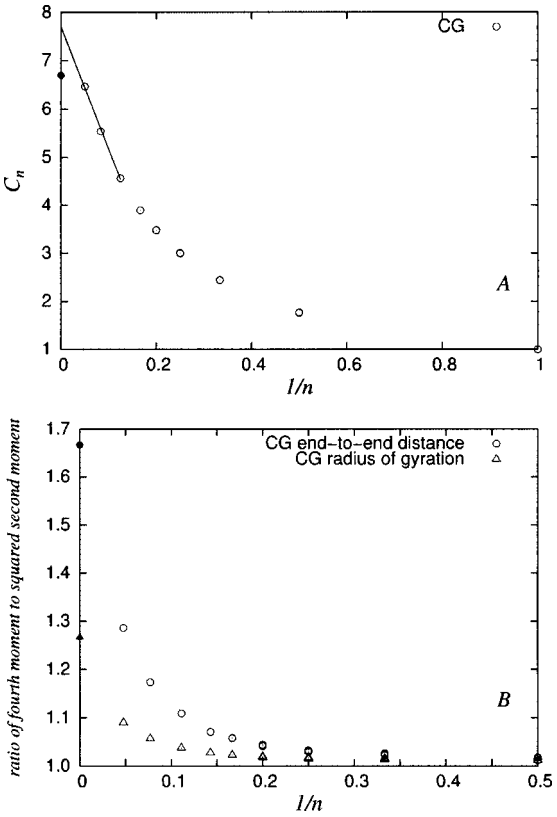

FIG. 6. (A) Characteristic ratio $C_n=\langle r^2\rangle/n\ell^2$, where r is the end-to-end distance, n is the number of bonds, and ℓ^2 is the mean square bond length. The data from the largest three systems is linearly extrapolated to $n\to\infty$. The limit of 7.7 is to be compared to the expected value for polyethylene of 6.7 (shown as a filled symbol). (B) $\langle r^4\rangle/\langle r^2\rangle^2$ and $\langle s^4\rangle/\langle s^2\rangle^2$ vs the inverse number of coarse grain sites, where r is the end-to-end distance and s is the radius of gyration. The expected theoretical values in the limit $n\to\infty$ are 5/3 and 19/15. These values are shown as filled symbols (Ref. 23).

equilibrium bond length, the bond force constant, and the two Lennard-Jones parameters, ϵ and σ, as follows. The sites are scaled so that the molecules have the correct mass. This is roughly, but not exactly, $1\pm 1/3n$ because of the extra hydrogen atoms at either end. The equilibrium bond length is scaled by $1\pm 1/3n$ and the bond force constant is scaled by $1\mp 1/3n$ since a longer bond should be less stiff. This scaling is in reasonable agreement with the AA data. The Lennard-Jones well depth should scale roughly as $1\pm 1/3n$ but comparison to the experimental data leads us to use $1\pm c/3n$ with $c=1.25$. The Lennard-Jones σ is weakly dependent on ϵ (see above) and is furthermore affected by all the other scaling. We correct for this dependence by scaling σ by $1\pm c/(3n)^2$ with $c=1.20$. The n^{-2} dependence makes this a minor adjustment, which is important because large variations in σ is what we are trying to avoid, in, for example, a polydisperse system.

V. RESULTS

The nonbonded CG parameters were fit against experimental bulk density and air/liquid surface tension data at 303 K. The results are shown in Fig. 2. To assess the behavior of quantities that were not directly fit into the model, we begin with the radius of gyration and the end-to-end distance. The mean squared radius of gyration and mean squared end-to-end distance versus alkane chain length are plotted in Fig. 3. The AA data are analyzed using the CG reduction procedure, wherein roughly every three carbon atoms and their hydrogen atoms are replaced with a single site (see Sec. III). The AA data analyzed in this fashion is in excellent agreement with the CG data. For a complete picture of the agreement, we look at the distribution of the radius of gyration and the end-to-end distance data for heptane, nonane, dodecane, tetradecane, and octadecane (see Figs. 4 and 5). The CG probability distributions are unimodal and are of the same width as the AA distributions. The AA distributions have more features, and in the case of heptane, are actually bimodal. This bimodal behavior arises because of the steric effect of the hydrogen atoms, which causes a preference for staggered and eclipsed conformations. These local preferences are averaged out for long chain length alkanes.

The limiting behavior of the mean squared radius of gyration and mean squared end-to-end distance is examined as the chain length becomes infinitely long. In Fig. 6(A) the characteristic ratio C_n is plotted versus $1/n$, where

$$C_n=\frac{\langle r^2\rangle}{n\ell^2}, \tag{4}$$

where r is the end-to-end distance, n is the number of bonds, and ℓ^2 is the mean square bond length. C_n approaches a limit as $n\to\infty$ which is linear in $1/n$; fitting a straight line to the data points corresponding to the largest three systems con-

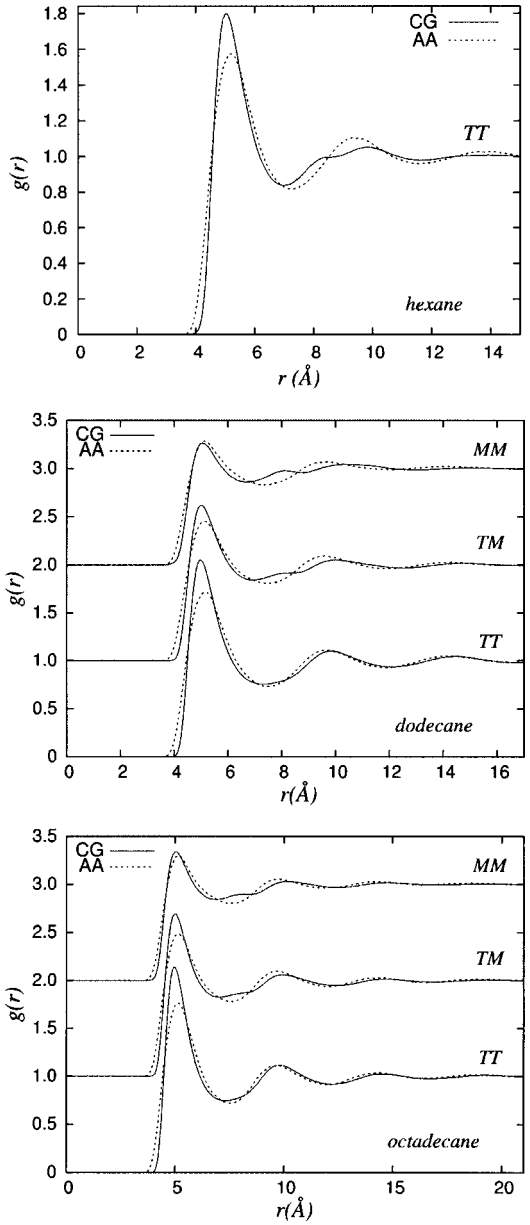

FIG. 7. The coarse grain and corresponding all-atom radial distribution functions for the terminal–terminal, terminal–middle, and middle–middle units of hexane, dodecane, and octadecane. Note that hexane does not contain any middle units, and that the *TM* and the *MM* curves are offset vertically by one and two units, respectively, for clarity.

sidered, we estimate the limit for the CG model to be 7.7. The expected value for polyethylene is 6.7. In Fig. 6(B) we plot the dimensionless ratios

$$\frac{\langle r^4\rangle}{\langle r^2\rangle^2} \quad \text{and} \quad \frac{\langle s^4\rangle}{\langle s^2\rangle^2} \tag{5}$$

versus the inverse number of coarse grain sites, where r is the end-to-end distance and s is the radius of gyration. The expected theoretical values[23] in the limit $n\to\infty$ are 5/3 and 19/15; extrapolation of the CG data to this limit shows excellent agreement. For the analysis performed in Fig. 6, there are duplicate and triplicate values corresponding to the representation of alkanes of differing chain length by the same number of CG sites. For example, in Fig. 6(A), $1/n=0.25$

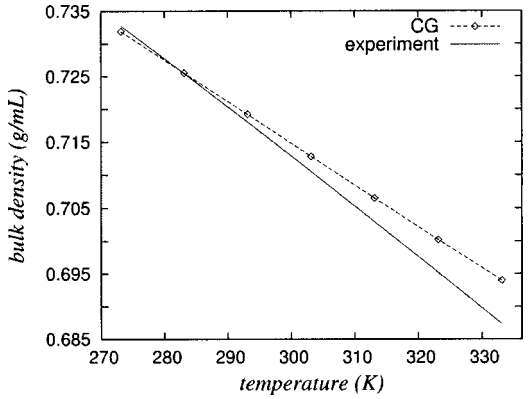

FIG. 8. Experimental and CG density of nonane as a function of temperature. The experimental data is in the form of an analytic fit by Rudek (Ref. 24).

corresponding to tetradecane, pentadecane, and hexadecane. The mean squared end-to-end distance and the mean squared bond length are different for these three alkanes, yet their characteristic ratios are not distiguishable on the scale of the plot. This property, which is also in evidence in Fig. 6(B), demonstrates that the scaling relations are physically reasonable.

The radius of gyration and end-to-end distance are properties of individual molecules. For an idea of how well the CG model captures the equilibrium structure of the bulk liquid, we turn to radial distribution functions; these were not used in the CG parameterization. The radial distribution functions for hexane, dodecane, and octadecane are shown in Fig. 7. To be able to compare the CG and AA data, the AA data is once again analyzed using the CG reduction procedure. The location of the first peak agrees in all cases. The remainder of the structure is correctly reproduced for the TT distribution for dodecane and octadecane. The agreement between the AA and CG data improves with increasing chain length as is expected.

We turn briefly to show the temperature dependence of the density of nonane in Fig. 8. The CG parameterization only made use of data at a temperature of 303 K. Nonetheless, the form of the intermolecular potential leads us to expect roughly the correct temperature dependence because condensed phase Lennard-Jones well depths are typically independent of temperature. For the range $273\,\mathrm{K}<T<333\,\mathrm{K}$, the density of nonane has a regression-fitted slope of $-7.565\times10^{-4}\,\mathrm{g\,cm^{-3}\,K^{-1}}$ for the experimental data which is in the form of an analytic fit by Rudek,[24] and a slope of $-6.32\times10^{-4}\,\mathrm{g\,cm^{-3}\,K^{-1}}$ for the CG model, an error of 16%. The current force field is valid in a narrow temperature range at room and physiological temperatures. In cases where a greater temperature range is desired, such as in polymer science, the parameterization scheme can be undertaken, separately, at different temperatures and the resulting CG potentials can be fit to include temperature dependence.[12]

Lastly, we look at the diffusion coefficients for single component alkane melts. No CG model to date has been parameterized using dynamical data,[14] and it is well known that parameterization using structural and thermodynamic properties results in diffusion coefficients which are too

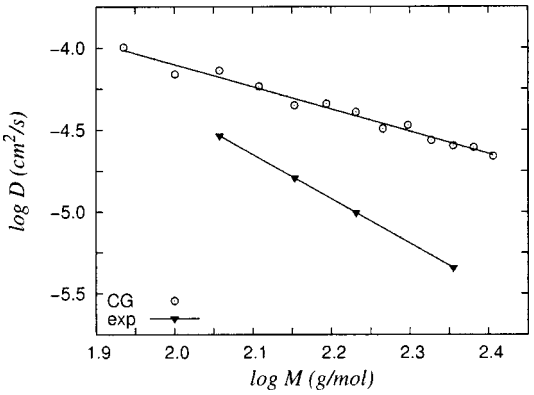

FIG. 9. Experimental (Ref. 25) and CG diffusion coefficients of linear alkanes at 303 K. Both sets of data are linear on a log–log scale, with a slope of −2.72 for the experimental data and −1.35 for the CG data.

high.[13,18] The soft intermolecular potentials which are responsible for the inflated diffusion are also responsible for being able to use a larger time step in integrating the equations of motion, and are a consequence of the reduced representation. Nonetheless, Whitehead[13] proposes using a CG model to study the diffusion of small molecules within a bilayer membrane. This could be accomplished by constructing a calibration curve between the CG diffusion coefficients and those obtained either from an AA membrane simulation or from experiment.[13] Experimental results establish that the diffusion coefficients of single component alkane melts are linear on a log–log scale when plotted against the molar mass.[25] The CG alkane data is also linear on this scale as shown in Fig. 9. The data in Fig. 9 can be used to gain a rough idea of the relationship between the CG simulation time and the actual time.

VI. CONCLUSIONS

A coarse grained model for *n*-alkanes was systematically developed using experimental bulk density and surface tension data. The model groups roughly three consecutive carbon atoms and their associated hydrogen atoms into one coarse grain site. To avoid unphysical behavior, scaling relations were introduced to spread the ''extra'' (i.e., the number of carbon atoms modulo three) atoms uniformly over the entire molecule. These relations are sufficiently general to allow for a description of alkanes of arbitrary length.

The model accurately reproduces the experimental bulk density and surface tension data for all linear alkanes at 303 K. The radius of gyration and end-to-end distance distributions agree quantitatively with all-atom molecular dynamics simulations, as do the radial distribution functions. In addition, the characteristic ratio and the ratio of the fourth moment of the radius of gyration and the fourth moment of the end-to-end distance to the square of the corresponding second moments agree well with the expected values in the limit of infinite chain length. The temperature dependence of the bulk density and the diffusion coefficients as a function of molar mass are also compared to experimental values.

In general there will be events occurring on a range of time scales, and even the relative ordering of these time scales is not *a priori* preserved in moving from a fully atomistic to a coarse grain representation. With enough physical insight, it is possible to construct models in which the time and length scales occurring in the coarse grain simulation are in the right proportions, as exemplified by the polyethylene melt model of Padding and Briels,[26] in which each coarse grain site represents 20 consecutive monomers.

The generality of the current model, in being of Lennard-Jones form, and the focus on interfacial data is anticipated to be well suited to our goal of improving upon a first generation coarse grain force field for aqueous amphiphilic systems.[19] The next task, consistent with this focus, is to obtain hydrocarbon/water nonbonded Lennard-Jones cross-parameters by fitting against experimental liquid–liquid interfacial tension data.

ACKNOWLEDGMENTS

This work was supported in part by a grant from the Natural Sciences and Engineering Research Council of Canada and the National Institutes of Health.

[1] A. Pralle, P. Keller, E.-L. Florin, K. Simons, and J. K. H. Hörber, J. Cell Biol. **148**, 997 (2000).
[2] G. Hummer and A. Szabo, Proc. Natl. Acad. Sci. U.S.A. **98**, 3658 (2001).
[3] D. A. Hendrix and C. Jarzynski, J. Chem. Phys. **114**, 5974 (2001).
[4] M. Ø. Jensen, S. Park, E. Tajkhorshid, and K. Schulten, Proc. Natl. Acad. Sci. U.S.A. **99**, 6731 (2002).
[5] H. L. Scott, Curr. Opin. Struct. Biol. **12**, 495 (2002).
[6] P. Lagüe, M. J. Zuckermann, and B. Roux, Biophys. J. **81**, 276 (2001).
[7] A. A. Louis, J. Phys.: Condens. Matter **14**, 9187 (2002).
[8] R. L. C. Akkermans and W. J. Briels, J. Chem. Phys. **114**, 1020 (2001).
[9] A. P. Lyubartsev and A. Laaksonen, Phys. Rev. E **52**, 3730 (1995).
[10] G. Tóth and A. Baranyai, J. Chem. Phys. **114**, 2027 (2001).
[11] J. D. McCoy and J. G. Curro, Macromolecules **31**, 9362 (1998).
[12] H. Fukunaga, J. Takimoto, and M. Doi, J. Chem. Phys. **116**, 8183 (2002).
[13] L. Whitehead, C. M. Edge, and J. W. Essex, J. Comput. Chem. **22**, 1622 (2001).
[14] F. Müller-Plathe, ChemPhysChem **3**, 754 (2002).
[15] J. C. Shelley, M. Y. Shelley, R. C. Reeder, S. Bandyopadhyay, and M. L. Klein, J. Phys. Chem. B **105**, 4464 (2001).
[16] J. C. Shelley, M. Y. Shelley, R. C. Reeder, S. Bandyopadhyay, P. B. Moore, and M. L. Klein, J. Phys. Chem. B **105**, 9785 (2001).
[17] C. F. Lopez, P. B. Moore, J. C. Shelley, M. Y. Shelley, and M. L. Klein, Comput. Phys. Commun. **147**, 1 (2002).
[18] C. F. Lopez, S. O. Nielsen, P. B. Moore, J. C. Shelley, and M. L. Klein, J. Phys.: Condens. Matter **14**, 9431 (2002).
[19] S. O. Nielsen and M. L. Klein, ''A coarse grain model for lipid monolayer and bilayer studies,'' in *Bridging the Time Scales: Molecular Simulations for the Next Decade*, edited by P. Nielaba, M. Mareschal, and G. Ciccotti (Springer, Berlin, 2002), pp. 27–63.
[20] J. A. Freites, Y. Choi, and D. J. Tobias, Biophys. J. **84**, 2169 (2003).
[21] J. T. Padding and W. J. Briels, J. Chem. Phys. **117**, 925 (2002).
[22] M. P. Allen and D. J. Tildesley, *Computer Simulations of Liquids* (Oxford University Press, Oxford, 1992).
[23] M. Fixman, J. Chem. Phys. **36**, 306 (1962).
[24] M. M. Rudek, J. A. Fisk, V. M. Chakarov, and J. L. Katz, J. Chem. Phys. **105**, 4707 (1996).
[25] E. von Meerwall, S. Beckman, J. Jang, and W. L. Mattice, J. Chem. Phys. **108**, 4299 (1998).
[26] J. T. Padding and W. J. Briels, J. Chem. Phys. **118**, 10276 (2003).